Supplement of Eur. J. Mineral., 35, 773–788, 2023
https://doi.org/10.5194/ejm-35-773-2023-supplement

European Journal of Mineralogy
Open Access

Supplement of

Metamorphic titanite–zircon pseudomorphs after igneous zirconolite

Cindy L. Urueña et al.

Correspondence to: Cindy L. Urueña (cindy.uruena@geol.lu.se)

Table S1. *Bulk-rock chemical composition of the melanocratic syenodiorite varieties. Sample CU19-09a: metamorphosed and undeformed syenodiorite. Sample CU19-09d: metamorphosed and deformed syenodiorite. CU19-09j: near-pristine igneous and undeformed syenodiorite.*

	%wt oxides														
Sample ID	**SiO_2**	**Al_2O_3**	**Fe_2O_3**	**CaO**	**MgO**	**Na_2O**	**K_2O**	**Cr_2O_3**	**TiO_2**	**MnO**	**P_2O_5**	**SrO**	**BaO**	**LOI**	**Total**
CU19-09a	54.3	18.15	8.4	5.38	1.97	4.56	3.57	0	1.63	0.22	1.12	0.07	0.45	1.24	101.06
CU19-09d	52	17.85	9.51	6.29	2.37	4.68	2.76	0	1.94	0.18	1.54	0.07	0.42	0.95	100.56
CU19-09j	53.5	18.45	8.28	6.01	2.03	4.81	3.08	0	1.67	0.21	1.27	0.07	0.36	0.32	100.06
	Traces in ppm														
Sample ID	**Ba**	**Ce**	**Cr**	**Cs**	**Dy**	**Er**	**Eu**	**Ga**	**Gd**	**Hf**	**Ho**	**La**	**Lu**	**Nb**	**Nd**
CU19-09a	392	163.5	10	0.3	9.78	4.89	6.33	23.9	13.2	4.6	1.8	86	0.57	12.6	89.8
CU19-09d	347	172.5	10	0.38	10.65	5.04	6.51	23.4	15.85	4.2	1.9	88.9	0.55	11.7	97.5
CU19-09j	297	159.5	10	0.23	9.52	4.88	6.3	23.6	13.65	4.8	1.82	86.3	0.55	13.6	88.6
Sample ID	**Pr**	**Rb**	**Sm**	**Sn**	**Sr**	**Ta**	**Tb**	**Th**	**Tm**	**U**	**V**	**W**	**Y**	**Yb**	**Zr**
CU19-09a	21.5	37	16.3	<1	665	0.4	1.8	1.35	0.61	0.33	40	138	55.1	3.54	204
CU19-09d	22.8	32.5	17.9	<1	664	0.4	2	1.11	0.64	0.28	48	221	54.9	3.65	183
CU19-09j	20.9	29.5	15.6	<1	708	0.5	1.78	1.31	0.62	0.31	36	255	53	3.74	195
	CIPW normative														
Sample ID	**Q**	**Or**	**Ab**	**An**	**Ac**	**Di**	**Wo**	**Hy**	**Ol**	**Il**	**Hm**	**Ttn**	**Ru**	**Ap**	**Sum**
CU19-09a	3	21.1	38.59	18.51	0	0	0	4.91	0	0.47	8.4	0.61	1.14	2.65	99.37
CU19-09d	1.9	16.31	39.6	19.55	0	0	0	5.9	0	0.39	9.51	1.13	1.28	3.65	99.21
CU19-09j	1.82	18.2	40.7	19.66	0	0	0	5.06	0	0.45	8.28	1.31	0.9	3.01	99.39

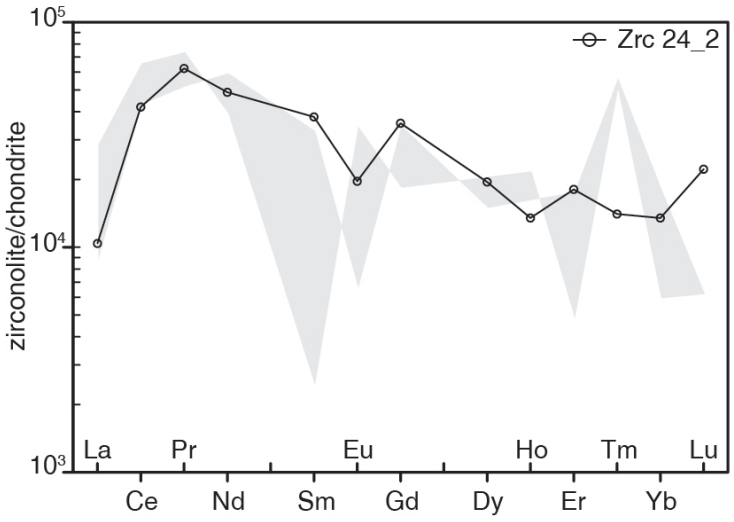

Figure S1. *Chondrite-normalised REE-pattern of the studied zirconolite in the near-pristine igneous syenodiorite. Black line for the representative analysis Zrc 24_2. In grey, data for the analyses Zrc 24_3 and 64-1 (not used for further calculations).*

Electron backscattered diffraction (EBSD) method

The EBSD technique enables the rapid and accurate identification of the crystallographic properties of the mineral (e.g., Stojakovic, 2012; Nickolsky and Yudintsev, 2021). The sample preparation included a final polish with 0.25 µm colloidal silica and a *c.* 5 nm thick carbon coating of the thin section to reduce diffraction interference and charging effects during EBSD analysis. EBSD data were collected using an Oxford Instrument AZtec system and a Nordlys detector integrated with the aforementioned FE-SEM instrument. The sample was mounted on a 70° tilted specimen holder and placed in the SEM chamber. Operation settings were a working distance of 17 mm, beam accelerating voltage at 20 kV, the band detection set to a minimum value of five, and various step sizes ranging between 20 to 200 nm were used during mapping. Other acquisition settings for electron backscatter diffraction patterns followed the methodology by Plan et al. (2021). Match units for indexing zirconolite diffraction patterns were selected from the AZtec database and were also created in the module *Twist* of the *HKL Channel5* software. Unit cell parameters of zirconolite-*2M* from Rossell (1980). Rossell (1980) provided the overall best-of-fit indexing solution. EBSD data were post-processed in the modules *Tango* and *Aztec Crystals* of the *HKL Channel5* software.

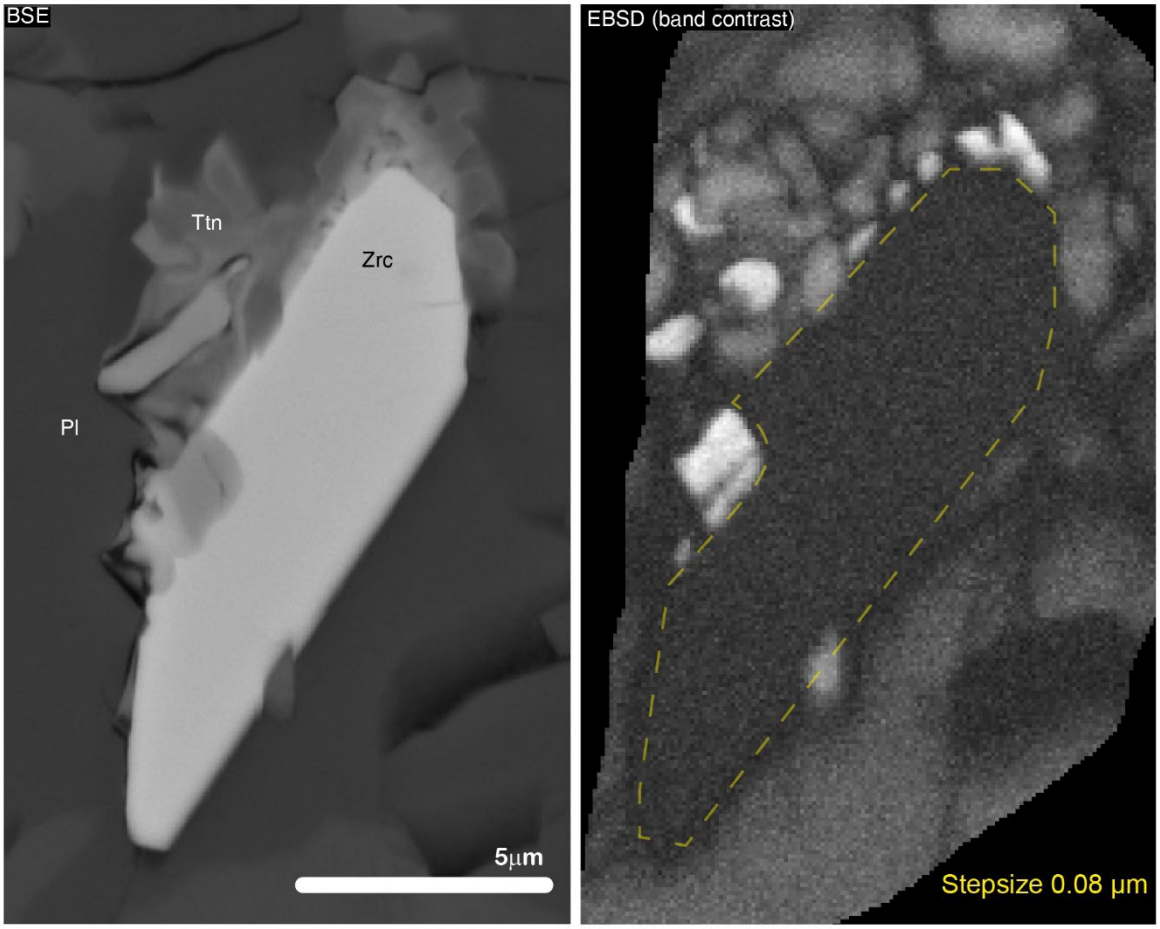

Figure S2. *Backscattered electron map of zirconolite crystal analysed by EBSD. Darker areas indicate poor and no Kikuchi patterns to be indexed. Areas in lighter colour (grey to white) corresponds to patterns that can be indexed.*

References

Nickolsky, M. S. and Yudintsev, S. V.: Electron Backscattered Diffraction for the Study of Matrices for Immobilization of Actinides Composed of the Murataite-Type Phases, Crystallogr. Reports 2021 661, 66, 130–141, https://doi.org/10.1134/S1063774521010090, 2021.

Plan, A., Kenny, G. G., Erickson, T. M., Lindgren, P., Alwmark, C., Holm-Alwmark, S., Lambert, P., Scherstén, A., and Söderlund, U.: Exceptional preservation of reidite in the Rochechouart impact structure, France: New insights into shock deformation and phase transition of zircon, Meteorit. Planet. Sci., 56, 1795–1828, https://doi.org/10.1111/MAPS.13723, 2021.

Rossell, H. J.: Zirconolite—a fluorite-related superstructure, Nature, 283, 282–283, https://doi.org/10.1038/283282a0, 1980.

Stojakovic, D.: Electron backscatter diffraction in materials characterization, Process. Appl. Ceram., 6, 1–13, 2012.